Random matrices, generalized zeta functions and self-similarity of zero distributions

2006 J. Phys. A: Math. Gen. 39 13983

(http://iopscience.iop.org/0305-4470/39/45/008)

INSTITUTE OF PHYSICS PUBLISHING JOURNAL OF PHYSICS A: MATHEMATICAL AND GENERAL

J. Phys. A: Math. Gen. **39** (2006) 13983–13997 doi:10.1088/0305-4470/39/45/008

Random matrices, generalized zeta functions and self-similarity of zero distributions

O Shanker

Bitfone Corporation, 32451 Golden Lantern Ste. 301, Laguna Niguel, CA 92677, USA

E-mail: oshanker@gmail.com

Received 23 August 2006, in final form 28 September 2006
Published 24 October 2006
Online at stacks.iop.org/JPhysA/39/13983

Abstract

There is growing evidence for a connection between random matrix theories used in physics and the theory of the Riemann zeta function and L-functions. The theory underlying the location of the zeros of these generalized zeta functions is one of the key unsolved problems. Physicists are interested because of the Hilbert–Polya conjecture, that the non-trivial zeros of the zeta function correspond to the eigenvalues of some positive operator. To complement the continuing theoretical work, it would be useful to study empirically the locations of the zeros by different methods. In this paper we use the rescaled range analysis to study the spacings between successive zeros of these functions. Over large ranges of the zeros the spacings have a Hurst exponent of about 0.095, using sample sizes of 10 000 zeros. This implies that the distribution has a high fractal dimension (1.9), and shows a lot of detailed structure. The distribution is of the anti-persistent fractional Brownian motion type, with a significant degree of anti-persistence. Thus, the high-order zeros of these functions show a remarkable self-similarity in their distribution, over fifteen orders of magnitude for the Riemann zeta function! We find that the Hurst exponents for the random matrix theories show a different behaviour. A heuristic study of the effect of low-order primes seems to show that this effect is a promising candidate to explain the results that we observe in this study. We study the distribution of zeros for L-functions of conductors 3 and 4, and find that the distribution is similar to that of the Riemann zeta functions.

PACS numbers: 02.70.Rr, 05.45.Df, 05.45.Pq

1. Introduction

The statistical distribution of the spacings of the zeros of the generalized zeta functions, including the Dirichlet L-functions, is of interest to mathematicians and physicists.

Mathematicians study the spacings because of its applications to analytic number theory, while physicists study it because of its relation to the theory of the spectra of random matrix theories (RMT) [1–4] and the spectra of classically chaotic quantum systems in physics. While many theoretical studies have been done and are being done, the relationship is incompletely understood, and it will be useful to augment our knowledge with empirical studies using several complementary approaches. In this paper we apply the widely utilized rescaled range analysis to numerically study the behaviour of the spacings. The analysis gives interesting insights into the asymptotic behaviour of the zero spacings. The paper is organized as follows. In section 2 we establish the required notation for the Riemann zeta function and L-functions. We also mention the observed relation to random matrix models and to studies of quantum chaology. In section 3 we introduce rescaled range analysis. The analysis is applied to the large height Riemann zeta zeros as calculated by Odlyzko [5]. We then apply it to the zeros of the Dirichlet L-functions at medium height, as calculated by Rubinstein [6]. In section 4 we discuss the empirical behaviour of the Hurst exponent for the Gaussian unitary ensemble (GUE). We also present a slightly different way of performing rescaled range analysis for the Riemann zeta zeros, which is more appropriate for comparison with the GUE results. In section 5 we give a brief introduction to quantum chaology and its implications for the possible role of the low-order primes in the study of the Riemann zeta zeros. We then consider heuristically the influence of the low-order primes on the behaviour of the Hurst exponent for the Riemann zeta zeros. In section 6 we give a brief summary of the results, and indicate the possible areas that would seem to be good candidates for further work.

2. Generalized zeta functions and random matrix models

In this section we establish the required notation for the Riemann zeta function and L-functions. We also mention the observed relation to random matrix models and to studies of quantum chaology.

The Riemann zeta function is defined for $\mathrm{Re}(s) > 1$ by

$$\zeta(s) = \sum_{n=1}^{\infty} n^{-s} = \prod_{p} (1 - p^{-s})^{-1}. \tag{1}$$

The product expression over the primes was first given by Euler. Equation (1) converges for $\mathrm{Re}(s) > 1$. It was shown by Riemann [7–10] that $\zeta(s)$ has a continuation to the complex plane and satisfies a functional equation

$$\xi(s) := \pi^{-s/2}\Gamma(s/2)\zeta(s) = \xi(1 - s); \tag{2}$$

$\xi(s)$ is entire except for simple poles at $s = 0$ and 1. Riemann multiplied the definition by $s(s - 1)$ to remove the poles. We write the zeros of $\xi(s)$ as $1/2 + \mathrm{i}\gamma$. The Riemann hypothesis asserts that γ is real for the non-trivial zeros. There is an impressive body of empirical evidence for this hypothesis, but a formal proof has been elusive. The numerical studies have found regions where the hypothesis is almost violated, but no counter-example has been found. A conjecture attributed to Hilbert and Polya is that the Riemann hypothesis is true because the non-trivial zeros of the zeta function are related to the eigenvalues of some positive operator. We order the γs in increasing order, with

$$\cdots \gamma_{-1} < 0 < \gamma_1 \leqslant \gamma_2 \cdots. \tag{3}$$

Then $\gamma_j = -\gamma_{-j}$ for $j = 1, 2, \ldots$, and $\gamma_1, \gamma_2, \ldots$ are roughly $14.1347, 21.0220, \ldots$. The remarkable properties of the Riemann zeta function can be generalized to a host of other zeta and L-functions. The simplest of the generalizations are for the Dirichlet L-functions $L(s, \chi)$

defined as follows: $q \geqslant 1$ is an integer and χ is a primitive character of the Abelian group formed by all integers smaller than and relatively prime to q. χ is extended to all integer values by making it periodic, and $\chi(m) = 0$ if m and q have a common factor. Then

$$L(s, \chi) = \sum_{n=1}^{\infty} \chi(n) n^{-s} = \prod_{p} (1 - \chi(p) p^{-s})^{-1}. \tag{4}$$

The analogue of the functional equation (2) is known for the generalized zeta functions, and they also seem to satisfy the generalized Riemann hypothesis. q is called the conductor of the L-function.

Odlyzko [5, 11] has made extensive numerical studies of the zeros of the Riemann zeta function and their local spacings. He also studied their relation to the random matrix models of physics. Wigner [1] suggested that the resonance lines of a heavy nucleus might be modelled by the spectrum of a large random matrix. Gaudin [3] and Gaudin-Mehta [2] gave results for the local (scaled) spacing distributions between the eigenvalues of typical members of the ensembles as $N \to \infty$, based on their study of orthogonal polynomials. Later Dyson [4] introduced the closely related circular ensembles.

Odlyzko confirmed numerically that the local spacings of the zeros of the Riemann zeta function obey the laws for the (scaled) spacings between the eigenvalues of a typical large unitary matrix. That is, they obey the laws of the Gaussian unitary ensemble (GUE) [1–4]. Katz and Sarnak [12] state that at the phenomenological level this may be the most striking discovery about zeta since Riemann. Odlyzko's computations thus verified the discoveries and conjectures of Montgomery [13–15]. We will discuss this further in section 5.

Further evidence for the connection between random matrices and generalized zeta functions comes from calculations of the zero correlation functions [16–19], and the study of the low-lying zeros of families of L-functions [20]. Extensive numerical computations [5, 6] have strengthened the connection.

Several authors [21–25] have studied the moments of the Riemann zeta function and families of L-functions, and the relation to characteristic polynomials of random matrices. The autocorrelation functions were studied in [26, 27]. The relation of the Riemann zeta function to probability laws was studied in [28].

It has been shown that the long-range statistics of the zeros of the Riemann zeta function are better described in terms of primes than by the GUE RMT. Berry [29–32] has related this to a study of the semiclassical behaviour of classically chaotic physical systems. The primitive closed orbits of the physical system are analogous to the primes p. We will expand on this further in section 5.

In what follows we apply the rescaled range analysis to study the distribution of the spacings $\delta_j = \gamma_{j+1} - \gamma_j$. For the zeros of the Riemann function we study four ranges of the spacings: δ_j for $1 \leqslant j \leqslant 10^5$, $10^{12} \leqslant j \leqslant 10^{12} + 10^4$, $10^{21} \leqslant j \leqslant 10^{21} + 10^4$, and $10^{22} \leqslant j \leqslant 10^{22} + 10^4$, using the zeros from the calculations of Odlyzko [5], and zeros around 35 161 820 using the calculations of Rubinstein [6]. For the Dirichlet L-functions of conductors 3 and 4 we use the zeros from the calculations of Rubinstein [6]. We selected these values because they are those which have zeros high enough that some of the asymptotic behaviour can be expected to occur.

Figure 1 shows a plot of the zero differences for zeros in the range $10^{12} \leqslant j \leqslant 10^{12} + 10^4$. One can see that the differences of the zeros jump around significantly, and the curve is noisy. The plot of the differences apparently has a large fractal dimension. Common measures for the fractal dimension are the Hausdorff dimension and the box dimension [33]. Rescaled range analysis usually gives the box dimension of a graph. For convenience we briefly state the definition of the box dimension. Let N_δ be the smallest number of boxes of side δ that

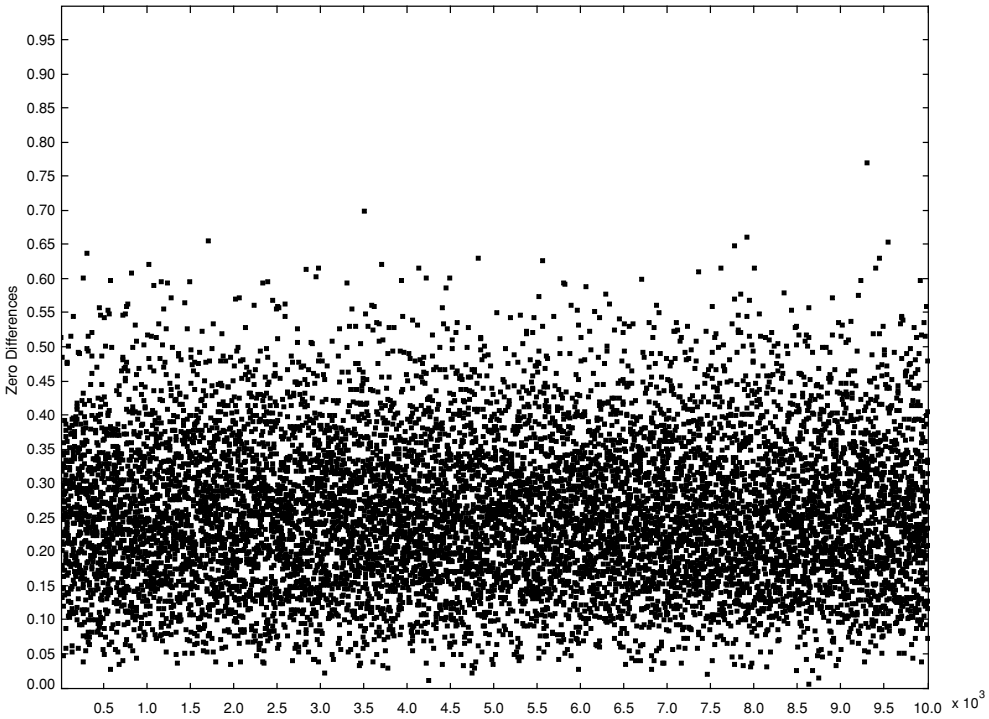

Figure 1. Differences of Riemann zeta zeros for zeros in the range $10^{12} \leqslant j \leqslant 10^{12} + 10^4$.

cover the graph F whose dimension we wish to measure. Then, as δ is made smaller, we will need more boxes to cover the graph. The limit

$$\mathrm{Lim}_{\delta \to 0} \frac{N_\delta}{-\log(\delta)}, \tag{5}$$

if it exists, is denoted as the box dimension of the graph F. For smooth graphs, this limit will be 1. If the graph is not smooth, then the limit would lie between 1 and 2.

3. Analysis of zero distributions for Riemann zeta and Dirichlet L-functions

In this section we introduce rescaled range analysis. The analysis is applied to the large height Riemann zeta zeros as calculated by Odlyzko [5]. We then apply it to the zeros of the Dirichlet L-functions at medium height, as calculated by Rubinstein [6]. We discuss the possible implications of the results of the analysis.

Rescaled range analysis [34–38] has been widely used to study series of observations which exhibit a combination of random (or pseudo-random) behaviour and regular behaviour. A good feel for rescaled range analysis can be developed by considering idealized Brownian motion in one dimension. Let $X(t)$ denote the position of a one-dimensional particle. Let the position get increments of constant magnitude and random sign at small time intervals τ. Then, as shown, for example, in Falconer [33], for timescales large compared to the kick interval τ, $X(t)$ has the following properties.

(i) With probability 1, $X(t)$ is a continuous function of t which is nowhere differentiable.
(ii) For any $t \geqslant 0$ and $h > 0$ (h large compared to kick interval), the increment $X(t+h) - X(t)$ is normally distributed with mean 0 and variance proportional to h. With suitable

normalization,

$$\text{Prob}(X(t+h) - X(t) \leqslant x) = (2\pi h)^{-1/2} \int_{-\infty}^{x} \exp(-u^2/2h)\, \mathrm{d}u. \tag{6}$$

(iii) If $0 \leqslant t_1 \leqslant t_2 \leqslant \cdots \leqslant t_{2m}$, the increments $X(t_2) - X(t_1), \ldots, X(t_{2m}) - X(t_{2m-1})$ are independent.

(iv) With probability 1, $X(t)$ has Hausdorff dimension and box dimension both equal to 1.5.

If the particle had a constant velocity in addition to the random kicks, the definition of $X(t)$ would be modified by subtracting out the uniform motion, so that the mean value of $X(t)$ would be still zero. Thus, $X(t)$ is the sum of a large number of independent and identically distributed random displacements, and the above results follow from the central limit theorem.

While Brownian motion graphs are of great theoretical importance, for practical applications one has to consider more general models [33]. A widely used generalization is fractional Brownian motion, in which the condition that successive increments should be independent is relaxed. A fractional Brownian motion of order α is defined similar to the Brownian motion, with the graph $X(t)$ having the following properties:

(i) With probability 1, $X(t)$ is a continuous function of t which is nowhere differentiable.

(ii) For any $t \geqslant 0$ and $h > 0$, the increment $X(t+h) - X(t)$ is normally distributed with mean 0 and variance proportional to $h^{2\alpha}$. With suitable normalization,

$$\text{Prob}(X(t+h) - X(t) \leqslant x) = (2\pi)^{-1/2} h^{-\alpha} \int_{-\infty}^{x} \exp(-u^2/2h^{2\alpha})\, \mathrm{d}u. \tag{7}$$

(iii) The increments $X(t+h) - X(t)$ and $X(t) - X(t-h)$ are not independent unless α is $1/2$. If $\alpha > 1/2$ then the increments tend to be of the same sign. If $\alpha < 1/2$ then the increments tend to differ in sign.

(iv) With probability 1, $X(t)$ has Hausdorff dimension and box dimension both equal to $2-\alpha$.

Rescaled range analysis makes use of equation (7) and determines the order of the fractional Brownian motion by studying how the vertical range X scales with the horizontal range h. The input to the analysis is a sequence of observations similar to that shown in figure 1.

It is common practice to denote the series of independent increments occurring in the rescaled range analysis by $\xi(t)$, where t is the ordinate of the observation. For our study, the series of increments are the differences of the zeros, which we have already denoted by δ_j. Rescaled range analysis studies the fractal dimension and correlations of the δ_j by boxing the observed data into bins of different sizes (the bin size being denoted by h), and by studying how the vertical range scales as the bin size h is varied. In our studies we have varied h from 32 to the maximum possible value allowed by the sample size. For each h, we calculated the R/S value for non-overlapping intervals (except for the end regions, where some overlap was necessary), and took the average. The estimated Hurst exponent obviously depends on the values of the bin size h that are considered, and on the maximum sample size. For large sample sizes the dependence is not very sensitive, for the data we have studied.

In terms of the mean value of δ_j for a given bin of size h, $\langle\delta\rangle$, the analysis defines $X(t)$ by

$$X(t) = \sum_{u=1}^{t} (\delta_u - \langle\delta\rangle). \tag{8}$$

Some remarks about equation (8) might be helpful. Firstly, we note that we subtract out the average value of δ for the given bin, which is appropriate because we are interested in the spread of the graph due to the random or quasi-random component. This is similar to subtracting out the uniform displacement due to a constant velocity of the particle in the Brownian motion

example above. Secondly, for the differences δ_j we have the relation that the sum of δ_j (δ_j is $\gamma_{j+1} - \gamma_j$) from a to b equals $\gamma_{b+1} - \gamma_a$. Thus, $X(t)$ for our study is equal to the tth difference of the zeros minus t times the average δ for the bin under consideration. This reflects the fact that $X(t)$ is a measure of the range of the graph. In particular, $X(h)$ is zero, where h is the size of the bin. The range R for the bin under consideration is defined as $\mathrm{Max}(X(t)) - \mathrm{Min}(X(t))$ where the maximum and minimum are taken for t between 1 and h, and S denotes the standard deviation of the δ_j for the chosen bin. It may be worthwhile to emphasize again that the quantities $X(t)$, R, S, $\langle\delta\rangle$, etc all depend on the bin under consideration.

As explained by Mandelbrot and Ness [39, 40], under quite general conditions, the dimensionless rescaled range R/S varies with h as $h \to \infty$ according to the scaling law

$$(R/S) = (ch)^{\alpha}, \tag{9}$$

where α is defined as the Hurst exponent. One can use linear regression analysis on a log–log plot of R/S against h to estimate the Hurst exponent α as the best fit slope of the log–log plot. The results of rescaled range analysis are summarized by the Hurst exponent. From the above discussion it follows that the Hurst exponent does not change if one adds the same constant value to δ_j or if one multiplies all δ_j by the same constant value, since one subtracts out the average value of δ_j in the analysis, and one scales the range using the standard deviation. Most natural phenomenon seems to have a value of about 0.7 for α.

If δ_j behave like normal Brownian motion, then the Hurst exponent is 0.5. Any deviation from this value implies that the values of the observable are not independent of each other. Mandelbrot introduced a generalized form of the Brownian motion model, the fractional Brownian motion [39, 40], as a typical simple family of random functions that models asymptotic dependence. In this model the Hurst exponent lies in the range $0 < \alpha < 1$. As mentioned earlier, the fractal dimension of the graph of the series of observations is given by $2 - \alpha$. A low value of α implies a large fractal dimension, namely, a curve which shows a lot of detailed structure. There are three types of generalized fractional Brownian motion: (a) the persistent, for values of α in the range $0.5 < \alpha < 1$, (b) the case $\alpha = 0.5$ which corresponds to the independent white noise processes of ordinary Brownian motion and (c) the anti-persistent, for $0 < \alpha < 0.5$. In the anti-persistent range any increasing trend in the past makes a decreasing trend in the future more probable, and vice versa. The strength of this anti-correlation depends on the extent to which α is lower than 0.5. The graph for an anti-persistent process shows a lot of jumps. We find that the spacings of the non-trivial zeros for all the zeta functions show a large degree of anti-persistence.

For completeness we mention that a persistent type of fractional Brownian motion implies that the increments' persistence is maintained over longer periods of time, depending on the excess of the Hurst exponent value over 0.5. If at some time in the past there was a positive increment i.e., an increase, it is more likely that there will be an increase in the future. A decreasing trend in the past implies the likelihood of a decreasing trend in the future.

Falconer [33] gives examples of other fractal curves which show a similar scaling of the vertical range with the horizontal range. Thus, the Hurst exponent that we are estimating is in essence a measure of the fractal structure of the zeros, and does not imply that the anti-correlation extends infinitely far.

For the zeros from the calculations of Odlyzko [5] we applied the rescaled range analysis to four sets of spacings of the zeros (δ_j): (a) $1 \leqslant j \leqslant 10^5$, (b) $10^{12} \leqslant j \leqslant 10^{12} + 10^4$, (c) $10^{21} \leqslant j \leqslant 10^{21} + 10^4$ and (d) $10^{22} \leqslant j \leqslant 10^{22} + 10^4$. For the range $1 \leqslant j \leqslant 10^5$ we found a Hurst exponent of about 0.8. However, in this range the R/S values did not scale according to equation (9). This is not surprising, since it is known that the distribution of zeros

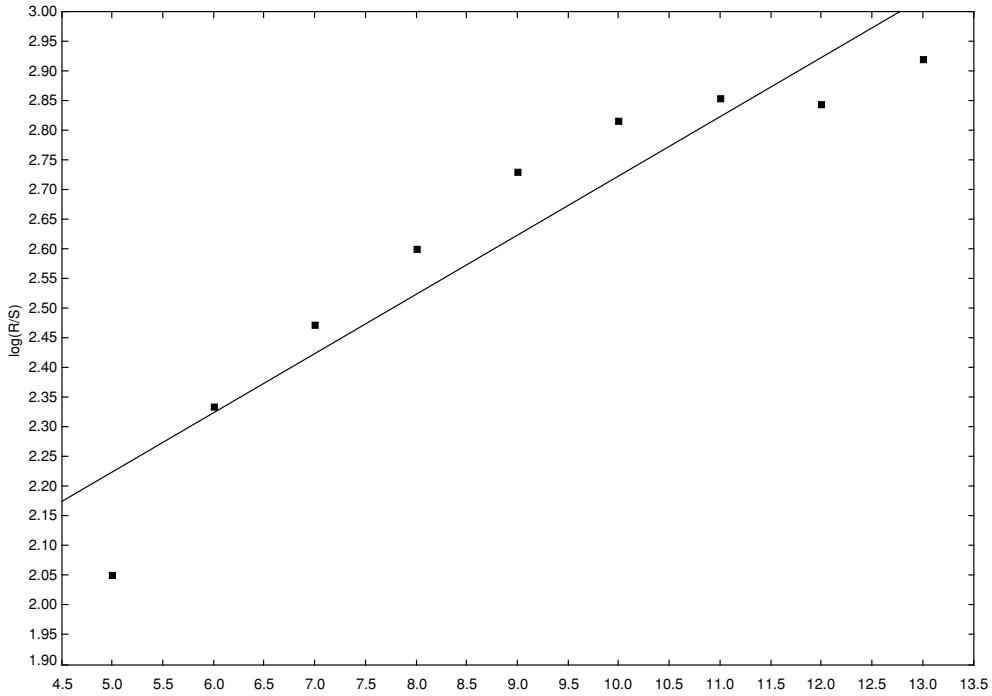

Figure 2. Hurst exponent estimate for Riemann zeta zeros in the range $10^{22} \leqslant j \leqslant 10^{22} + 10^4$.

Table 1. Hurst exponent for high-order Riemann zeros, sample size 10 000.

Range of zeros	Hurst exponent	Standard error
$10^{12} \leqslant j \leqslant 10^{12} + 10^4$	0.093	0.007
$10^{21} \leqslant j \leqslant 10^{21} + 10^4$	0.094	0.012
$10^{22} \leqslant j \leqslant 10^{22} + 10^4$	0.100	0.013

reaches its asymptotic behaviour very slowly. This is related to the slow rate of growth of the function $S(t)$, defined by

$$S(t) := \pi^{-1} \arg \zeta\left(\tfrac{1}{2} + it\right). \tag{10}$$

We therefore do not consider this region further in our rescaled range analysis. Table 1 shows the results of the analysis for the remaining three ranges of the zeros.

One can see that the Hurst exponent is remarkably constant over fairly wide values of the range of zeros. The low value of the exponent is interesting. It implies that there is a large degree of anti-persistence. This means that the differences of the zeros jump around significantly, leading to a noisy curve. The plot of the differences shows a large fractal dimension (see figure 1).

Figure 2 shows the regression analysis for zeros in the range $10^{22} \leqslant j \leqslant 10^{22} + 10^4$. The horizontal axis is the log of the bin size ($\log_2(h)$), and the vertical axis is the log of the mean R/S ($\log_2(R/S)$) for the given values of h. The slope of the best fit line gives the value of the Hurst exponent. The best fit line is also shown in the figure. The data is fairly linear.

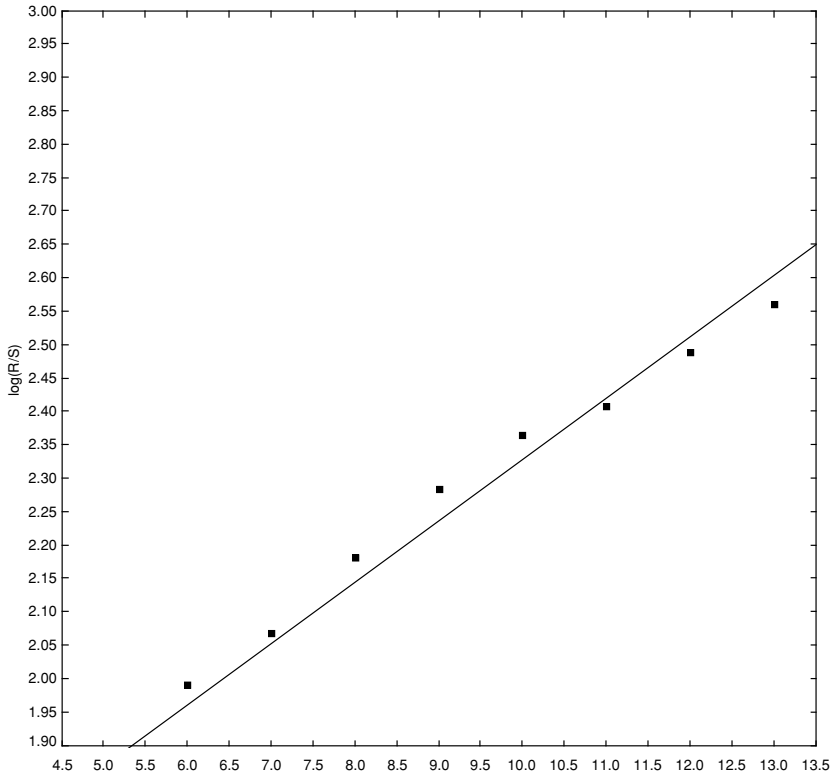

Figure 3. Hurst exponent estimate for zeros of Dirichlet L-function of conductor 4.

Table 2. Hurst exponent for L-functions, sample size 100 000.

Order of largest zero studied	Function	Hurst exponent	Standard error
35 161 820	Riemann zeta	0.091	0.004
31 712 310	Conductor 3	0.092	0.007
32 457 680	Conductor 4	0.092	0.007

For lower values of h the scaling behaviour is not expected to hold, since it an asymptotic phenomenon.

Table 2 shows the results of the analysis for the Dirichlet L-functions. The sample size used in all the cases reported in the table is 100 000 zeros. Figure 3 shows the regression analysis for zeros of the L-function of conductor 4. As before, the horizontal axis is the log of the bin size ($\log_2(h)$), and the vertical axis is the base 2 log of the mean R/S ($\log_2(R/S)$) for the given values of h. The best fit line is also shown in the figure. The results of the analysis for the L-functions are remarkably similar to the results for the Riemann zeta function.

Since the application of the rescaled range analysis has led to such interesting results, one can ask what the implications are for the physics and the mathematics of the study of the Riemann zeta function. As was discussed in section 2, two important topics which help explain many properties of the zeta zero distributions are random matrix theory and the effect of low-order primes. We will discuss these in separate sections. In the next section we

compare the results for the Riemann zeta function at large heights with the behaviour of the Hurst exponent for matrices chosen from the GUE.

4. Comparison with random matrix theory

In this section we discuss the empirical behaviour of the Hurst exponent for the GUE. We also present a slightly different way of performing rescaled range analysis for the Riemann zeta zeros, which is more appropriate for comparison with the GUE results.

To do the numerical investigations we need to determine the appropriate size N of the matrices in the GUE. The matrix size N is usually taken to be such that the mean eigenvalue spacings for the matrices and for the zeta function zeros at the desired height γ are equal. Asymptotically, for the Riemann zeta function the mean number of zeros with height less than γ (the smoothed Riemann zeta staircase) is [10]

$$\langle \mathcal{N}_{\mathcal{R}}(\gamma) \rangle = (\gamma/2\pi)(\ln(\gamma/2\pi) - 1) - \tfrac{7}{8}. \tag{11}$$

Thus, the mean spacing of the zeros at height γ is $2\pi(\ln(\gamma/2\pi))^{-1}$. The mean spacing of the eigenvalues for the GUE is $2\pi/N$, where N is the matrix size. Thus, the statistics of the zeta zeros at height γ are to be compared with the RMT for matrices of size $N = \ln(\gamma/2\pi)$. We choose the zeta zeros in the range $10^{22} \leqslant j \leqslant 10^{22} + 10^4$ for the comparison. γ is 1.37×10^{21} for the zeros in this range, and hence N is 47. We recall that for the zeta zeros in this range, we found a Hurst exponent of 0.1 when we used all the available zeros, which gave us a sample size of 10 000 points. However, for the GUE the eigenvalues come in blocks of size N, and hence it is not obvious what is the proper way to compare the results. One way is to generate a set of matrices from the GUE (fixing the matrix size as discussed above), calculate the Hurst exponent for each of them, and get the distribution of the Hurst exponents for the different matrices. One can then also break the Riemann zeros in the range into blocks of N zeros and generate the distribution of the Hurst exponents for these blocks. The small sample size makes the uncertainties in the estimated exponent much larger than is the case for the estimate using the full sample size. Since $N = 47$ is much smaller than the full sample size of 10 000, the mean Hurst exponent for the zeta zeros calculated in this manner will be different from the value 0.1 that we found earlier. Of course the value which was determined using the full range is more accurate, but it may not be the appropriate value to use for comparing with the GUE results.

When we calculate the Hurst exponents for the Riemann zeros by breaking them into blocks of N zeros, we find that the mean Hurst exponent for the Riemann zeros is 0.34 for blocks of size 47. The mean Hurst exponent for the GUE matrices of size 47 is 0.65. If we recall our discussion of the Hurst exponent, we see that this is a significant difference. We must emphasize that the right way to compare the GUE results with the Riemann zeta zero analysis is not clear. To work with reasonably large matrices, we would need to be able to compute zeros much higher on the critical line than we are currently able to do. Thus, the results of this analysis have to be treated with caution, but this is probably the best that we can do. We varied the block size from 40 to 51, and found that the mean Hurst exponent for the Riemann zeros in the range $10^{22} \leqslant j \leqslant 10^{22} + 10^4$ varied between 0.33 and 0.34. The GUE mean value showed variation from 0.58 for $N = 40$ to 0.70 for $N = 51$. The two ranges of variation are not directly comparable, and we merely present the variations to give the reader some idea of the variability. In order to verify that the Hurst exponent distribution for the zeta zeros is insensitive to the range chosen for study, we calculated the mean Hurst exponent for Riemann zeros covering the range $10^{21} \leqslant j \leqslant 10^{21} + 10^4$. For a block size of 47 we found the mean exponent to be 0.33. We may mention that the Hurst exponents for the GUE RMT

behave similarly to the spectra for the adjacency matrices of complex networks, which we had investigated in a separate study.

One may wonder if relaxing the condition that the mean matrix eigenvalue spacing be equal to the mean zeta zero spacing, and going to larger matrix sizes, will reduce the discrepancy found above. We numerically studied the Hurst exponent for matrices of size 100, and found that the discrepancy becomes worse. Thus, in spite of the ambiguities in comparing the GUE results with the Riemann zeta results, the differences in the behaviour seem significant enough that the RMT is disfavoured as an explanation for the results found in our zeta zero analysis.

For completeness we should remark that as the block size is increased, the distribution of the Hurst exponents for the Riemann zeta zeros becomes quite narrow, and settles down to the constant values reported in earlier sections. An interesting topic for further research would be the theoretical study of the Hurst exponent in the GUE as the matrix size $N \to \infty$. The joint probability distributions for the GUE eigenvalues [41] $\lambda_1 \geqslant \lambda_2 \cdots \geqslant \lambda_N$ is

$$2^{N(N-1)/2} \exp\left(-\sum \lambda_i^2\right) \prod_{i<j} (\lambda_i - \lambda_j)^2 \Bigg/ \left(\pi^{N/2} \prod_{i=1}^{N} \Gamma(i)\right). \tag{12}$$

Edelman [41] shows that for large N the eigenvalues approach the zeros of the Hermite polynomial of order N. This may be a promising direction to take in studying the problem. In the next section we study the effect of the low-order primes.

5. Effect of the low-order primes

In this section we give a brief introduction to quantum chaology and its implications for the possible role of the low-order primes in the study of the Riemann zeta zeros. We then consider heuristically the influence of the low-order primes on the behaviour of the Hurst exponent for the Riemann zeta zeros. We try to identify which aspect of the correspondence with quantum chaology might shed some light on the low Hurst exponents that we observe for the Riemann zeta zeros.

Quantum chaology is defined by Berry [31] as the study of semiclassical, but non-classical, behaviour characteristic of systems whose classical motion exhibits chaos. By semiclassical one means the limit as Planck's constant $\hbar \to 0$. The distribution of eigenvalues of quantum chaotic systems shows universality [29–32]. The universality class depends on the symmetries of the system's Hamiltonian. For systems without time-reversal invariance the distribution of eigenvalue spacings approaches that of the GUE. The connection between quantum chaology and the Riemann zeta function comes about because the Riemann hypothesis would follow if the imaginary parts γ_j of the non-trivial zeros of the Riemann zeta function are eigenvalues of a self-adjoint operator. The relation of the zeta zero differences to the GUE, that we reviewed in section 2, seems to indicate that the still-unknown dynamical operator (if one exists) would not have time-reversal symmetry and would have a classical limit which is chaotic.

Let us denote the Riemann staircase, the number of zeros with height less than some value γ, by $\mathcal{N}_{\mathcal{R}}(\gamma)$. Thus,

$$\mathcal{N}_{\mathcal{R}}(\gamma) = \sum_{j=1}^{\infty} \Theta(\gamma - \gamma_j), \tag{13}$$

where Θ denotes the unit step function. Further evidence for the connection between quantum chaology and the Riemann zeta function comes from the study of the fluctuations of $\mathcal{N}_{\mathcal{R}}(\gamma)$

from the smooth approximation $\langle \mathcal{N}_{\mathcal{R}}(\gamma)\rangle$ in equation (11). The fluctuating part of the Riemann staircase function can be written as [30]

$$\mathcal{N}_{R,osc}(\gamma) = \mathcal{N}_{\mathcal{R}}(\gamma) - \langle \mathcal{N}_{\mathcal{R}}(\gamma)\rangle = -\frac{1}{\pi}\lim_{\eta\to 0}\mathrm{Im}\ln\zeta\left(\frac{1}{2} - \mathrm{i}(\gamma + \mathrm{i}\eta)\right). \tag{14}$$

If we use the product form of equation (1) in equation (14) (ignoring for the moment the question of how to truncate the asymptotic divergent product when equation (1) is used on the critical line. See [30] for a discussion), we get

$$\mathcal{N}_{R,osc}(\gamma) = -\frac{1}{\pi}\sum_{p}\sum_{m=1}^{\infty}\sin(m\gamma\ln p)/(mp^{m/2}) \tag{15}$$

where the label p indicates a sum over the primes. For a quantum chaotic system a very similar formula can be written down for the fluctuating part of the spectral staircase (the function which counts the number of eigenvalues less than a given energy E). For quantum chaological systems the spectral staircase fluctuation formula follows from the semiclassical approximation, where the eigenvalue density fluctuations can be expressed in terms of the actions related to closed orbits. Berry [30] refers to the underlying theory by the intriguing term Ouroborology. Ouroboros was a mythical snake that swallowed its tail, and the term symbolizes the constructive interference of quantum waves associated with classical orbits. Thus, one can set up a formal analogy between fluctuations of the Riemann staircase and fluctuations of the spectral staircase of a classically chaotic system. In particular, one can associate primitive closed orbits of the hypothesized dynamical system with the primes p. The actions of the closed orbits are

$$S_{pm} = m\gamma\ln p. \tag{16}$$

The semiclassical limit corresponds to $\gamma\to\infty$. The instability exponents for the closed orbits (independent of the energy, i.e., height γ) are

$$\lambda_p = \ln p. \tag{17}$$

The periods of the closed orbits would be

$$T_{pm} = m\ln p. \tag{18}$$

In section 2 we had mentioned Montgomery's results [14], that the statistics of the Riemann zeta zeros are those of the GUE. The theorem proved by Montgomery concerns the form factor $K(\tau)$ of the zeros; this is the Fourier transform of the pair correlation function, defined as

$$K(\tau) = \lim_{M\to\infty}\left(\frac{1}{M}\sum_{j=1}^{M}\sum_{k=1}^{M}\exp(2\pi\mathrm{i}\tau(x_j - x_k)) - \frac{\sin(M\pi\tau)}{\pi\tau}\right), \tag{19}$$

where x_j are the rescaled Riemann zeros, scaled so as to have unit mean spacing. Montgomery proved that $K(\tau)$ was $|\tau|$ for $|\tau| < 1$, and he conjectured that $K(\tau)$ would be 1 for $|\tau| > 1$, as it is for the form factor in the GUE. This once again strengthens the connection between the Riemann zeta function and dynamical quantum chaotic systems.

In section 2 we had mentioned the close agreement of Odlyzko's calculations with Montgomery's theorem. Odlyzko found good overall agreement for $K(\tau)$ with the GUE predictions, but he did find that the $K - K_{\mathrm{GUE}}$ reveals a series of spikes for small τ. Such spikes are predicted by the semiclassical theory, which shows deviations from universality for

large energy scales, that is short time scales [29]. For $|\tau| < 1$ the semiclassical formula for $K(\tau)$, expressed in terms of the closed-orbit amplitudes and periods, is

$$K(\tau) = \pi^2\tau^2 \sum_p \sum_{m=1}^{\infty} B_{pm}^2 \delta(\tau - T_{pm}/(2\pi\hbar\langle d\rangle)), \tag{20}$$

where $\langle d\rangle$ is the average density of eigenvalues, and B_{pm} is an amplitude term. In the semiclassical limit $\hbar \to 0, \hbar\langle d\rangle$ scales as $\hbar^{-(D-1)}$ for a system with D degrees of freedom ($D > 1$), so in that limit the spike associated with a given orbit slides towards $\tau = 0$. For any finite τ the spikes are thickly clustered in the semiclassical limit, and it is their average which gives the $K = |\tau|$ behaviour. But an accurate evaluation of $K(\tau)$ should reveal at least the first few spikes. In the Riemann zeta case equation (18) shows that spikes should occur at τ-values proportional to the logarithms of powers of primes. This is precisely the behaviour observed by Odlyzko. We investigate heuristically here whether these characteristic spikes could play a role in the small Hurst exponent that we observe.

We now follow closely the treatment in [44] of the Fourier transform of the zero differences. In the remaining part of this section we will follow the notation of [44] to the extent feasible. Odlyzko empirically observed long-range correlations between the Riemann zeta zero differences δ_j. To understand these correlations, he studied the spectrum of the zero differences, in particular, he studied

$$f(x) = c \left| \sum_{n=N}^{N+M} (\delta_n - \langle\delta\rangle)\, \mathrm{e}^{\mathrm{i}\pi n x} \right|^2, \tag{21}$$

where c is a constant, x is the transform variable, and the values for N and M are 10^{12} and 98 303, respectively. He observed very sharp peaks in $f(x)$ for x near $2(\log N)^{-1} \log q$, where q is a prime power. He related these spikes to the formulae that connect zeros of the zeta function and prime numbers. In particular, he used the formula of Landau [42, 43], that for any $y > 0$ as $N \to \infty$,

$$\sum_{n=1}^{N} \mathrm{e}^{\mathrm{i}\gamma_n y} = -(\gamma_N/(2\pi)) \exp(-y/2) \log(p) + O(\exp(-y/2)\log(N)) \tag{22}$$

if $y = \log(p^m)$ where p is a prime and m is an integer, and

$$\sum_{n=1}^{N} \mathrm{e}^{\mathrm{i}\gamma_n y} = O(\exp(-y/2)\log(N)) \text{ otherwise.} \tag{23}$$

If we define $h(y) = \sum_{n=N+1}^{N+M} \mathrm{e}^{\mathrm{i}\gamma_n y}$, then $h(y)$ will be large precisely in the vicinity of $\log p^m$ and small elsewhere. Let us write

$$\gamma_{N+k} = \gamma_N + ka + \beta_k, \tag{24}$$

where a is the average spacing $2\pi(\ln(\gamma_N/2\pi))^{-1}$. Odlyzko refers to a as α, but we already use α for the Hurst exponent. The β_k are usually small, on the order of $1/a$. For y small one can write $h(y) = \mathrm{e}^{\mathrm{i}\gamma_N y} \sum_{k=1}^{M} \mathrm{e}^{\mathrm{i}kay + i\beta_k y}$, or approximately

$$h(y) = \mathrm{e}^{\mathrm{i}\gamma_N y} \sum_{k=1}^{M} \mathrm{e}^{\mathrm{i}kay} + iy\, \mathrm{e}^{\mathrm{i}\gamma_N y} \sum_{k=1}^{M} \beta_k\, \mathrm{e}^{\mathrm{i}kay}. \tag{25}$$

The first sum on the right-hand side of equation (25) is small for y away from integer multiples of $2\pi/a$, so it is the second term that contributes the oscillations at $y = \log p^m$. On the other hand, one can approximately write

$$\sum_{n=N+1}^{N+M} (\delta_n - \langle\delta\rangle)\, \mathrm{e}^{\mathrm{i}\pi n x} = a^{-1} \sum_{n=N+1}^{N+M} (\gamma_{n+1} - \gamma_n - a)\, \mathrm{e}^{\mathrm{i}\pi n x}, \tag{26}$$

or,

$$\sum_{n=N+1}^{N+M} (\delta_n - \langle\delta\rangle)\, \mathrm{e}^{\mathrm{i}\pi nx} = a^{-1}\, \mathrm{e}^{\mathrm{i}\pi Nx} \sum_{k=1}^{M} (\beta_{k+1} - \beta_k)\, \mathrm{e}^{\mathrm{i}\pi kx}. \tag{27}$$

A simple manipulation of equation (27) shows that it is proportional to $\sum_{k=1}^{M} \beta_k\, \mathrm{e}^{\mathrm{i}\pi kx}$, and hence the Fourier transform of the zero differences can be expected to behave like the second term on the right-hand side of equation (25), and to have large peaks whenever $x = (a/\pi) \log p^m$ for primes p and $m \geqslant 1$.

To see if the characteristic sharp peaks in the Fourier transform of the zeta zero differences at powers of the prime numbers could explain the low Hurst exponent that we observe, we inverted a Fourier transform which has large peaks at 2, 3, 4, 5, 7, 8, 9, 11, 13, 16, 17 and 19, and we calculated the Hurst exponent for the sequence thus obtained. We used the value $N = 10^{12}$ and $M = 10^4$, and we found Hurst exponents in the range 0.04–0.20 (depending on the sharpness of the assumed peaks), compared to the value 0.09 that we got from the Riemann zero differences. Thus, low-order primes seem to be a promising avenue to understand the results that we observe in this study. Further work on this topic would be useful.

In the next section we give a brief summary of the results, and indicate the possible areas that would seem to be good candidates for further work.

6. Conclusions

Our study for the Riemann zeta function gave a variation in the Hurst exponent from 0.091 to 0.1 for zeros covering the range 10^7 to 10^{22}, for sample sizes of 10 000 zeros. This shows that there is a significant amount of self-affinity in the distribution of the zeros. It is quite intriguing that the distribution for different zeta functions at the intermediate range of zeros also shows values for the Hurst exponent which are very close to the values found for the Riemann function zeros. We find that the GUE RMT apparently has a different behaviour from the Riemann zeros. However, it is not obvious how the comparison between the GUE and the Riemann zeta zeros is to be made.

One can see that the Hurst exponent is remarkably constant for the different zeta functions. The low value of the exponent is interesting. It implies that there is a large degree of anti-persistence. This means that the differences of the zeros jump around significantly, leading to a noisy curve. The plot of the differences shows a large fractal dimension, about 1.9.

In conclusion, we mention some possible consequences of the above investigation. The results that we observe seem to indicate that the influence of the low-order primes on the Hurst exponent for the zeta zeros may be a promising candidate for further study. The behaviour of the Hurst exponent in the GUE for large matrix sizes is another area which might benefit from further research. This study considered the Hurst exponent for Dirichlet L-functions, but the main concentration was on the Riemann zeta function. A more detailed look at the Hurst exponent for the zero differences of the Dirichlet L-functions might also be useful.

Acknowledgments

The author is grateful to Charles Ryavec, David Farmer, Michael Berry and Andrew Odlyzko for their comments and suggestions. The author is responsible for any shortcomings or errors in this work.

References

[1] Wigner E 1967 Random Matrices in Physics *SIAM Rev.* **9** 1–23
[2] Gaudin M and Mehta M 1960 On the density of eigenvalues of a random matrix *Nucl. Phys.* **18** 420–7
[3] Gaudin M 1961 Sur la loi Limite de L'espacement de Valuers Propres D'une Matrics Aleatiore *Nucl. Phys.* **25** 447–58
[4] Dyson F 1962 Statistical theory of energy levels III *J. Math. Phys.* **3** 166–75
[5] Odlyzko A 1989 The 10^{20}-th zero of the Riemann zeta function and 70 million of its neighbors (preprint) A.T.T
[6] Rubinstein M 1998 Evidence for a spectral interpretation of zeros of L-functions *PhD Thesis* Princeton University
[7] Riemann B 1858 Über die Anzahl der Primzahlen uter Einer Gegebenen Gröbe *Montasb. der Berliner Akad.* **160** 671–80
[8] Riemann B 1892 *Gesammelte Werke* (Leipzig: Teubner)
[9] Titchmarsh E 1986 *The Theory of the Riemann Zeta Function* 2nd edn (Oxford: Oxford University Press)
[10] Edwards H M 1974 *Riemann's Zeta Function* (New York: Academic)
[11] Odlyzko A 2001 Dynamical, spectral, and arithmetic zeta functions *(Contemporary Math. series* vol 290*)* (Providence, RI: American Mathematical Society) pp 139–44
[12] Katz N M and Sarnak Peter 1999 Zeroes of zeta functions and symmetry *Bull. Am. Math. Soc.* **36** 1–26
[13] Montgomery H 1971 *Topics in Multiplicative Number Theory Lecture Notes in Mathematics* vol 227 (Berlin: Springer)
[14] Montgomery H 1973 The pair correlation of zeroes of the zeta function *Proc. Sym. Pure Math.* vol 24 (Providence, RI: American Mathematical Society) pp 181–93
[15] Goldston D and Montgomery H 1987 Pair correlation of zeros and primes in short intervals *Progress in Math.* vol 70 (Basle: Birkhauser) pp 183–203
[16] Hejhal D A 1994 On the triple correlation of zeros of the zeta function *Int. Math. Res. Not.* **7** 293–302
[17] Rudnick Z and Sarnak P 1996 Principal L-functions and random matrix theory *Duke Math. J.* **81** 269–322
[18] Bogomolny E B and Keating J P 1995 Random matrix theory and the Riemann zeros: I. Three- and four-point correlations *Nonlinearity* **8** 1115–31
[19] Bogomolny E B and Keating J P 1996 Random matrix theory and the Riemann zeros: II. n-Point correlations *Nonlinearity* **9** 911–35
[20] Katz N M and Sarnak P 1999 *Random Matrices, Frobenius Eigenvalues and Monodromy* (Providence, RI: American Mathematical Society)
[21] Keating J P and Snaith N C 2000 Random matrix theory and $\zeta(1/2+it)$ *Commun. Math. Phys.* **214** 57–89
[22] Keating J P and Snaith N C 2000 Random matrix theory and L-functions at $s = 1/2$ *Commun. Math. Phys.* **214** 91–110
[23] Conrey J B and Farmer D W 2000 Mean values of L-functions and symmetry *Int. Math. Res. Not.* **17** 883–908 (*Preprint* math.nt/9912107)
[24] Hughes C P, Keating J P and O'Connell N 2000 Random matrix theory and the derivative of the Riemann zeta function *Proc. R. Soc.* A **456** 2611–27
[25] Hughes C P, Keating J P and O'Connell N 2001 On the characteristic polynomial of a random unitary matrix *Commun. Math. Phys.* **220** 429–51
[26] Conrey J B, Farmer D W, Keating J P, Rubinstein M O and Snaith N C 2002 Integral moments of zeta- and L-functions *Preprint* math.nt/0206018
[27] Conrey J B, Farmer D W, Keating J P, Rubinstein M O and Snaith N C 2003 Autocorrelation of random matrix polynomials *Commun. Math. Phys.* **237** 365–95
[28] Biane P, Pitman J and Yor M 2001 Probability laws related to the Jacobi theta and Riemann zeta functions, and Brownian motion *Bull. Am. Math. Soc.* **38** 435–65
[29] Berry M V 1985 Semiclassical theory of spectral rigidity *Proc. R. Soc.* A **400** 229–51
[30] Berry M V 1986 Riemann's zeta function: a model for quantum chaos? *Quantum Chaos and Statistical Nuclear Physics (Springer Lecture Notes in Physics* vol 263*)* pp 1–17
[31] Berry M V 1987 Quantum chaology *Proc. R. Soc.* A **413** 183–98
[32] Berry M V 1988 Number variance of the Riemann zeros *NonLinearity* **1** 399–407
[33] Falconer K 2003 *Fractal Geometry: Mathematical Foundations and Applications* 2nd edn (New York: Wiley)
[34] Hurst H E 1951 Long term storage capacity in reservoirs *Trans. Am. Soc. Civ. Eng.* **116** 770–99
[35] Feller W 1966 *Introduction to Probability Theory and its Applications* (New York: Wiley)
[36] Feder J 1991 *Fractals* (New York: Plenum)
[37] Peters E E 1991 *Chaos and Order in the Capital Markets* (New York: Wiley)
[38] Pallikari F and Boller E 1999 A rescaled range analysis of random events *J. Sci. Explor.* **13** 25–40

[39] Mandelbrot B B and Van Ness J 1968 *SIAM Rev.* **10** 422–37
[40] Mandelbrot B B 1982 *The Fractal Geometry of Nature* (San Francisco: Freeman)
[41] Edelman A 1989 Eigenvalues and Condition Numbers of Random Matrices *PhD Thesis* Massachusetts Insititute of Technology
[42] Landau E 1911 U:ber die Nullstellen der Zetafunktion *Math. Ann.* **71** 548–64
[43] Gonek S M 1985 A formula of Landau and mean values of $zeta(s)$ *Topics in Analytic Number Theory* ed S W Graham and J D Vaaler (Austin, TX: University of Texas Press) pp 92–7
[44] Odlyzko A 1987 On the distribution of spacings between zeros of the zeta function *Math. Comp* **48** 273–308